# EFFICIENT COMPUTATION OF SOUND ABSORPTION IN PANEL STRUCTURES WITH POROUS CAVITIES

**Nicolas Roy [(1)], Sylvain Germès [(2)]**

*[(1)] Top Modal, 130 rue Galilée, Labège, France Email: nicolas.roy@topmodal.fr*
*[(2)] Saint-Gobain Research Compiègne, Thourotte, France, Email: sylvain.germes@saint-gobain.com*

**KEYWORDS**

e.g. structural dynamics, fluid-structure coupling, porous cavities, sound transmission loss

**ABSTRACT**

The optimal design of structures in terms of noise attenuation is of great importance in many fields including aerospace, automotive, naval and the construction industry. Panel structures with relatively large surfaces and low mass are especially prone to vibroacoustic excitation thus requiring extensive simulation and testing during the design phase in order to meet performance goals.

A normal mode approach has been formulated and implemented to perform analysis of panel structures with porous cavities in order to predict and improve their sound transmission loss (STL).

The resulting method has been integrated in a user-friendly interactive tool. Additional features include the computation of the modal contributions to the total radiated power as well as the spatial contribution of the radiating surface elements to the total power.

## 1. INTRODUCTION

Coupled fluid-structure analysis typically involves a BEM/FEM (Boundary Element Method and Finite Element Method) approach that combines a fluid domain model (BEM) and a structural model (FEM) to solve the fully coupled vibroacoustic problem.

Several commercial packages exist; however, their use can require substantial computational resources and therefore may not be well adapted to the specific needs of preliminary design and optimization.

In an earlier study [1], a simpler alternative method was considered to represent a diffuse field acting on a panel structure by the use of modal joint acceptance functions [2]. This method was implemented and interfaced with a finite element code in order to perform efficient vibroacoustic responses of structures subjected to a diffuse sound field. Comparison of the results with BEM/FEM analysis and experimental measurements showed very good correlation.

Recently a new study has been performed with Saint-Gobain in order to expand the previous method to the computation of the sound absorption of panel structures with porous cavities. The sound absorption is expressed using the Sound Transmission Loss (STL) defined as the ratio of the incident power to the radiated power as a function of frequency. In order to maintain computational efficiency, the incident diffuse field is again represented by an equivalent blocked pressure excitation using the joint acceptance functions, and the radiated sound is determined using the Rayleigh integral. This results in a modal approach without the need for explicit boundary elements.

The porous cavities are taken into account by first modeling them explicitly using 3D (non-porous) fluid finite elements after which the corresponding mass and stiffness matrices are condensed using the normal modes of the fluid cavities. Finally, the porous material properties are introduced into the modal mass and stiffness matrices using equivalent fluid model theory.

In this paper the underlying methods related to the computation of the STL and the modeling of the porous cavities are described. Next the implementation in the PRIMODAL software tool is presented. Finally, an industrial application is presented to illustrate the interest of the tool in the context of preliminary design and optimization.

## 2. THEORY

### 2.1. Sound Transmission Loss

The sound transmission loss is illustrated using the schematic test setup depicted in Fig. 1.

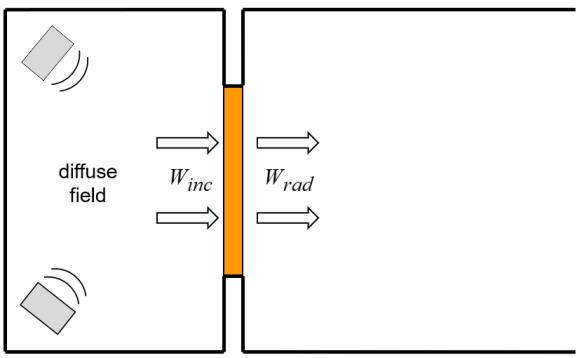


*Figure 1: Setup for determining STL of Panel*

The panel shown in orange is mounted in an opening between a source room on the left and a receiver room on the right. A diffuse field in the source room is used to excite one side of the panel.

The sound transmission loss (STL) defined in Eq. 1 is used to characterize the sound absorption of the panel. It is a unitless term expressing in dB the ratio of the incident power $W_{inc}$ to the radiated (transmitted) power $W_{rad}$.

$$STL = 10 \log\left(\frac{W_{inc}}{W_{rad}}\right) \quad (1)$$

### 2.2. Diffuse Field

A diffuse sound field [3] can be defined as a field with uniform sound pressure $p$ with no privileged direction of propagation. As a result, the diffuse field can be characterized in the frequency domain in terms of its pressure autospectral density function $S_p(\omega)$.

Furthermore, it can be shown that the spatial correlation $\gamma_{ij}$ between two points $i$ and $j$ in the diffuse field can be expressed by the following relation with $k = \omega / c$ the acoustic wave number and $a$, the distance between the two points.

$$\gamma_{ij} = \frac{\sin(ka)}{ka} \quad (2)$$

Following the development provided by Coyette [4], the incident pressure $p_i$ acting on the surface of the panel has an autospectral density function $S_{p_i}(\omega)$ which is half of $S_p(\omega)$ since the related spatial integral is limited to a half-space instead of the full space

$$S_{p_i} = \frac{1}{2} S_p \quad (3)$$

The autospectral density of incident power is given by the following expression where $A$ is the total area of the panel's surface, and $\rho$ and *c* the mass density and speed of sound of the acoustic medium.

$$S_{W_{inc}}(\omega) = \frac{S_{p_i}(\omega)}{4\rho c} A = \frac{S_p(\omega)}{8\rho c} A \quad (4)$$

The excitation pressure is approximated by the blocked pressure $p_b$ which is the sum of the incident and scattered pressure components acting on the panel assumed to be motionless. Near the surface of the panel the blocked pressure is approximately twice the value of the incident pressure thus leading to the following relations between the corresponding autospectral densities

$$S_{p_b} = 4 S_{p_i} \quad (5)$$

Finally, from Eqs. 4 and 5 we can express the autospectral density of the incident power in terms of the autospectral density of the blocked pressure.

$$S_{W_{inc}}(\omega) = \frac{S_{p_b}(\omega)}{16\rho c} A \quad (6)$$

### 2.3. Computation of STL

#### *2.3.1. Random Excitation*

The diffuse acoustic field is represented by an equivalent force PSD matrix $\mathbf{S}_F$ applied to the discretized points (nodes) of the incident side of the panel as defined below where $\mathbf{A}$ is a diagonal matrix of nodal areas, $\boldsymbol{\gamma}$ the symmetric spatial correlation matrix using Eq. 2 and $S_{p_b}$ the blocked pressure autospectral density function.

$$\mathbf{S}_F = \mathbf{A}\boldsymbol{\gamma}\mathbf{A} \cdot S_{p_b} \quad (7)$$

Instead of using Eq. 7 directly, the physical forces $\mathbf{F}$ are converted to the generalized forces $\mathbf{F}_k$ using the normal modes $\boldsymbol{\Phi}$ of the structure according to the transformation in Eq. 8.

$$\mathbf{F}_k = \boldsymbol{\Phi}^T \mathbf{F} \quad (8)$$

This leads to the expression in Eq. 9 where the diffuse field is now represented by a PSD matrix of *generalized* forces $\mathbf{S}_{F_k}$. The main advantage of the modal transformation is the reduction in size especially when the number of modes is much less than the number of nodes.

$$\mathbf{S}_{F_k} = \boldsymbol{\Phi}^T (\mathbf{A}\boldsymbol{\gamma}\mathbf{A})\boldsymbol{\Phi} \cdot S_{p_b} \quad (9)$$

#### *2.3.2. Mechanical Mobility*

In order to compute the random response of the panel the matrix of mechanical mobilities $\mathbf{Y}$ (velocity/force) between the *generalized* forces $\mathbf{F}_k$ and the nodal velocities on the *radiating* side of the panel are required. The mobilities are computed using a modal approach which takes into account the presence of porous cavities. The introduction of porous cavities is detailed later. The matrix $\mathbf{Y}$ is complex valued with rows relative to the velocities and columns relative to the generalized forces.

#### *2.3.3. Acoustic Resistance Matrix*

The acoustic resistance matrix $\mathbf{R}$ is the real part of the acoustic impedance matrix $\mathbf{Z}$. The acoustic impedance matrix is computed using the Rayleigh integral [5 – 7]. The method is based on the analysis of a flat circular piston of area $dS$ lying in an infinite baffle and moving harmonically with a velocity amplitude of $v_0$. The total acoustic pressure $p$

produced by the motion of the piston on another area $dS'$ can be determined by the Rayleigh integral defined below where $r$ is the distance between $dS$ and $dS'$.

$$p = \iint \frac{i\rho ck}{2\pi R} v_0 e^{-ikR} dS \qquad (10)$$

The total reaction force $f_r$ acting on $dS'$ is given by

$$f_r = -p\, dS' \qquad (11)$$

from which the acoustic impedance $\mathbf{Z}$ can be defined as follows.

$$Z = \frac{-f_r}{v_0} \qquad (12)$$

The acoustic resistance matrix is obtained by the discretization of the radiating surface [8]. Each node of the radiating surface is assumed to move as a rigid circular piston. This discretization requires that the size of each nodal piston defined by its equivalent radius, $r$, must be much smaller than the acoustic wavelength ($k\,r \ll 1$) and the structural wavelength.

Using this approach, the values for the diagonal ($R_{ii}$) and off-diagonal ($R_{ij}$) terms of $\mathbf{R}$ are given by

$$R_{ii} = \rho c S_i \left[ 1 - \frac{J_1(2k\,r_i)}{k\,r_i} \right] \qquad (13)$$

$$R_{ij} = \frac{2\rho c k^2 S_i S_j}{\pi} \left[ \frac{J_1(k\,r_i)}{k\,r_i} \frac{J_1(k\,r_j)}{k\,r_j} \right] \mathrm{sinc}(k\,r_{ij}) \qquad (14)$$

where $S_i$ and $S_j$ are the surfaces of the equivalent pistons, $r_i = \sqrt{S_i/\pi}$ and $r_j = \sqrt{S_j/\pi}$ the corresponding radii, $r_{ij}$ the distance between the pistons (nodes), and $J_1$ the Bessel function of order 1.

*2.3.4.Radiated Power*

From the previously defined terms, the expression for the autospectral density of the radiated power can be defined by the following expression.

$$S_{W_{rad}}(\omega) = \frac{1}{2} \sum \mathrm{diag}(\mathbf{R}\,\mathbf{Y}\,\mathbf{S}_{F_k}\,\mathbf{Y}^*) \qquad (15)$$

Note that $S_{W_{rad}}$ is real-valued and positive since both $\mathbf{R}$ and the product $(\mathbf{Y}\,\mathbf{S}_{F_k}\,\mathbf{Y}^*)$ are real positive matrices.

Finally, the sound transmission loss *STL* can be determined by introducing Eqs. 15 and 6 in Eq. 1.

*2.3.5.Contributions to Radiated Power*

The autospectral density function $S_{W_{rad}}$ in Eq. 15 can also be expressed as the sum of the terms of the matrix $\mathbf{W}$ defined below where the symbol $\otimes$ designates the term by term product of the two matrices and conj($\mathbf{Y}$) refers to the complex conjugate of $\mathbf{Y}$ *without* transpose.

$$\mathbf{W} = \frac{1}{2} \Re \left[ (\mathbf{R}\,\mathbf{Y}\,\mathbf{S}_{F_k}) \otimes \mathrm{conj}(\mathbf{Y}) \right] \qquad (16)$$

This leads to the following equivalent expression for $S_{W_{rad}}$.

$$S_{W_{rad}}(\omega) = \sum_i \sum_j W_{ij} \qquad (17)$$

Although Eqs. 15 and 17 are equivalent, Eq. 17 is numerically more efficient to compute because it avoids the computation of the cross-spectral terms which are not used.

Another advantage of the matrix $\mathbf{W}$ in Eq. 17 is that in can be used to identify the contributing components in terms of the modes or the zones (nodes) of the vibrating surface.

Notice that the rows of $\mathbf{W}$ correspond to the nodes of the radiating surface and that the columns correspond to the structural modes. Therefore, by summing $\mathbf{W}$ over the rows we obtain the participation of each mode $j$ to the total radiated power.

$$W_j(\omega) = \sum_i W_{ij} \qquad (18)$$

We can define normalized modal contributions by dividing the $W_j(\omega)$ by the incident power $W_{inc}(\omega)$.

$$\tau_j(\omega) = W_j(\omega) / W_{inc}(\omega) \qquad (19)$$

Similarly, by summing over the columns of $\mathbf{W}$, we obtain the contribution of each node $i$ to the total radiated power.

$$W_i(\omega) = \sum_j W_{ij} \qquad (20)$$

It is important to note that the above power contributions are real-valued but can be negative. However, their sum will always be positive and equal to the total radiated power.

$$\sum_i W_i(\omega) = \sum_j W_j(\omega) = S_{W_{rad}}(\omega) \qquad (21)$$

## 2.4. Porous Material

### *2.4.1. Introduction*

The panel structure under consideration may contain one or several acoustic cavities with porous materials. The following assumptions apply to the acoustic cavities:

- All acoustic cavities are modelled explicitly with 3D fluid elements
- The same porous material (or simple fluid such as air) is common to all the acoustic cavities
- Porous materials are represented by an equivalent fluid model with frequency dependent properties

The theory used to derive the equivalent fluid model is outlined below.

### *2.4.2. Equivalent Fluid Model*

A rigid porous formulation is considered which assumes a perfectly rigid behavior of the skeleton (solid phase) of the porous material. This leads to an equivalent fluid model with the dynamic mass density and dynamic bulk modulus expressed below where $\rho_f$ and $K_f$ are the mass density and bulk modulus of the fluid phase of the porous material

$$\rho(\omega) = \rho_f \ \alpha(\omega) \qquad (22)$$

$$K(\omega) = K_f \ / \beta(\omega) \qquad (23)$$

The Johnson model is used to define the dynamic tortuosity $\alpha(\omega)$ according to the following expression [9,10].

$$\alpha(\omega) = \alpha_\infty \left( 1 + \frac{1}{jx} \sqrt{1 + \frac{M}{2} jx} \right) \qquad (24)$$

$$\text{with } x = \frac{\omega \rho_f \ \alpha_\infty}{\sigma \phi} \text{ and } M = \frac{8 k_0 \ \alpha_\infty}{\phi \Lambda^2} \qquad (25)$$

and

| | | |
|---|---|---|
| $\alpha_\infty$ | = | tortuosity |
| $\phi$ | = | porosity |
| $\sigma$ | = | resistivity |
| $\Lambda$ | = | viscous characteristic length |
| $k_0$ | = | viscous permeability $\eta / \sigma$ |
| $\eta$ | = | viscosity |

The Champoux and Allard model is used to define the dynamic compressibility $\beta(\omega)$ according to the following expression [9, 10].

$$\beta(\omega) = \gamma - \frac{\gamma - 1}{1 + \frac{1}{jx'} \sqrt{1 + \frac{M'}{2} jx'}} \qquad (26)$$

$$\text{with } x' = \frac{\omega \rho_f \ k_0' \ P_r}{\eta \phi} \text{ and } M' = \frac{8 k_0'}{\phi \Lambda'^2} \qquad (27)$$

and

| | | |
|---|---|---|
| $\gamma$ | = | ratio of specific heats $C_p / C_v$ |
| $P_r$ | = | Prandtl number $\eta C_p / \kappa$ |
| $\kappa$ | = | thermal conductivity |
| $\Lambda'$ | = | thermal characteristic length |
| $k_0'$ | = | thermal permeability ( $k_0' = \phi \Lambda'^2 / 8$ ) |

As an illustration, the equivalent fluid properties $\rho(\omega)$ and $c(\omega)$ for a 45 mm thick glass wool cavity are plotted below in Fig. 2. Note that the properties are now frequency-dependent and complex-valued thus introducing dissipation to the model.

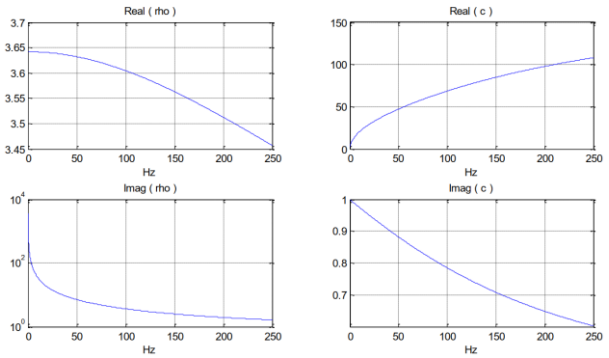


*Figure 2: Equivalent Fluid Model Properties*

## 2.5. Coupled Fluid-Structure Analysis

The equations of motion governing the harmonic response of a structure comprising $s$ DOF coupled with one or more fluid cavities comprising $f$ DOF are expressed below.

$$\left( -\omega^2 \begin{bmatrix} \mathbf{M}_{ss} & \mathbf{0}_{sf} \\ -\mathbf{C}_{fs} & \mathbf{M}_{ff}(1/K_0) \end{bmatrix} + \begin{bmatrix} \mathbf{K}_{ss} & \mathbf{C}_{sf} \\ \mathbf{0}_{fs} & \mathbf{K}_{ff}(1/\rho_0) \end{bmatrix} \right) \begin{bmatrix} \mathbf{u}_s \\ \mathbf{p}_f \end{bmatrix} = \begin{bmatrix} \mathbf{F}_s \\ \mathbf{0}_f \end{bmatrix} \qquad (28)$$

with

| | |
|---|---|
| $\mathbf{M}_{ss}$ | Structure mass matrix (symmetric) |
| $\mathbf{K}_{ss}$ | Structure stiffness matrix (symmetric) |
| $\mathbf{M}_{ff}$ | Fluid "mass" matrix (symmetric) |
| $\mathbf{K}_{ff}$ | Fluid "stiffness" matrix (symmetric) |
| $\mathbf{C}_{fs}$ | Coupling matrix ( $\mathbf{C}_{sf} = \mathbf{C}_{fs}^T$ ) |
| $\mathbf{u}_s$ | Vector of structural displacements |
| $\mathbf{p}_f$ | Vector of fluid pressures |
| $\mathbf{F}_s$ | Vector of forces applied to the structure |

The uncoupled normal modes of the structure and fluid are obtained by solving the following eigenvalue problems.

$$(-\omega_n^2 \mathbf{M}_{ss} + \mathbf{K}_{ss})\mathbf{\Phi}_{sk} = \mathbf{0}_s \qquad (29)$$

$$(-\omega_m^2 \mathbf{M}_{ff} + \mathbf{K}_{ff})\mathbf{\Phi}_{fl} = \mathbf{0}_f \qquad (30)$$

Using the uncoupled modes from Eqs. 29 and 30, the physical system of Eq. 28 can be condensed to the generalized (modal) displacements leading to the following system of equations.

$$\left(-\omega^2 \begin{bmatrix} \mathbf{m}_k + \mathbf{M}_{res} & \mathbf{0}_{kl} \\ -\mathbf{C}_{lk} & \mathbf{m}_l \end{bmatrix} + \begin{bmatrix} \mathbf{k}_k & \mathbf{C}_{kl} \\ \mathbf{0}_{lk} & \mathbf{k}_l \end{bmatrix}\right)\begin{bmatrix} \mathbf{q}_k \\ \mathbf{q}_l \end{bmatrix} = \begin{bmatrix} \mathbf{f}_k \\ \mathbf{0} \end{bmatrix} \qquad (31)$$

with

| | |
|---|---|
| $\mathbf{m}_k$ | Structure matrix of generalized masses |
| $\mathbf{M}_{res}$ | Residual mass matrix of fluid |
| $\mathbf{k}_k$ | Structure matrix of generalized stiffnesses |
| $\mathbf{m}_l$ | Fluid matrix of generalized masses |
| $\mathbf{k}_l$ | Fluid matrix of generalized stiffnesses |
| $\mathbf{C}_{lk}$ | Condensed coupling matrix ( $\mathbf{C}_{kl} = \mathbf{C}_{lk}^T$ ) |
| $\mathbf{q}_k$ | Structure generalized displacements |
| $\mathbf{q}_l$ | Fluid generalized displacements |
| $\mathbf{f}_k$ | Structure generalized forces |

The residual mass matrix $\mathbf{M}_{res}$ represents the mass of the truncated fluid modes projected onto the structural modes. It is obtained using the following expression.

$$\mathbf{M}_{res} = \mathbf{\Phi}_{ks}\,\mathbf{C}_{sf}\,\mathbf{G}_{ff,res}\,\mathbf{C}_{fs}\,\mathbf{\Phi}_{sk} \qquad (32)$$

The term $\mathbf{G}_{ff,res}$ in Eq. 32 is the matrix of residual flexibility of the fluid which can be obtained by the following system involving the fluid stiffness matrix augmented by the fluid modes.

$$\begin{bmatrix} \mathbf{K}_{ff} & \mathbf{M}_{ff}\,\mathbf{\Phi}_{fl} \\ \mathbf{\Phi}_{lf}\,\mathbf{M}_{ff} & \mathbf{0}_{ll} \end{bmatrix}\begin{bmatrix} \mathbf{G}_{ff,res} \\ \boldsymbol{\lambda}_l \end{bmatrix} = \begin{bmatrix} \mathbf{I}_{ff} \\ \mathbf{0}_{ll} \end{bmatrix} \qquad (33)$$

The presence of porous materials introduces frequency-dependent terms in the equations of motion of Eq. (31) leading to the following system of equations

$$\left(-\omega^2 \begin{bmatrix} \mathbf{m}_k + \mathbf{M}_{res}/c_k(\omega) & \mathbf{0}_{kl} \\ -\mathbf{C}_{lk} & c_m(\omega)\mathbf{m}_l \end{bmatrix} + \begin{bmatrix} \mathbf{k}_k & \mathbf{C}_{kl} \\ \mathbf{0}_{lk} & c_k(\omega)\mathbf{k}_l \end{bmatrix}\right)\begin{bmatrix} \mathbf{q}_k \\ \mathbf{q}_l \end{bmatrix} = \begin{bmatrix} \mathbf{f}_k \\ \mathbf{0} \end{bmatrix} \qquad (34)$$

where $c_m$ and $c_k$ are unitless correction coefficients for the fluid generalized mass and stiffness matrices given by

$$c_k(\omega) = \frac{\rho_0}{\rho(\omega)} \qquad c_m(\omega) = \frac{K_0}{K(\omega)} \qquad (35)$$

The terms $\rho_0$ and $K_0$ in Eq. 35 correspond to the reference values of the fluid mass density and bulk modulus used to obtain the fluid modes in Eq. 30. The equivalent fluid properties $\rho(\omega)$ and $K(\omega)$ are defined in Eqs. 22 and 23.

The equations of motion shown in Eq. 34 are undamped. Damping in the structure may be included via structural damping. This results in a structural damping matrix $\mathbf{H}_{kk}$ (generally coupled) which is added to the diagonal matrix of generalized stiffnesses as an imaginary term.

In the fluid, if a porous material is used, damping is included in the complex-valued fluid properties $\rho(\omega)$ and $K(\omega)$. If a non-porous fluid such as air is used, global structural damping in the fluid $\eta_f$ may be specified.

This leads to the final damped equations of motion for the coupled fluid-structures system in Eq. 36.

$$\left(-\omega^2 \begin{bmatrix} \mathbf{m}_k + \mathbf{M}_{res}/c_k(\omega) & \mathbf{0}_{kl} \\ -\mathbf{C}_{lk} & c_m(\omega)\mathbf{m}_l \end{bmatrix} + \begin{bmatrix} \mathbf{k}_k + i\,\mathbf{H}_{kk} & \mathbf{C}_{kl} \\ \mathbf{0}_{lk} & c_k(\omega)\mathbf{k}_l(1+i\,\eta_f) \end{bmatrix}\right)\begin{bmatrix} \mathbf{q}_k \\ \mathbf{q}_l \end{bmatrix} = \begin{bmatrix} \mathbf{f}_k \\ \mathbf{0} \end{bmatrix} \qquad (36)$$

## 3. IMPLEMENTATION

### 3.1. Introduction

The STL computation of panel structures with porous material has been implemented using the NASTRAN finite element code along with the PRIMODAL structural analysis code. The overall procedure is shown in Fig. 3 and described hereafter.

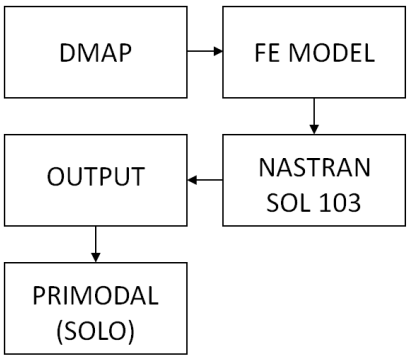


*Figure 3: STL Implementation Flowchart*

### 3.2. NASTRAN Analysis

The NASTRAN input file is configured using a normal mode approach (SOL 103) with additional entries for creating complementary output data needed for the STL post-processing in PRIMODAL.

The input file contains both the panel structure and fluid cavities. The fluid cavity material entry (MAT10) is written with the reference values for $\rho_0$ and $K_0$.

The incident and radiating surfaces of the structure are defined using two PLOAD entries. The PLOAD entry with the smallest ID corresponds to the incident surface and the PLOAD with the largest ID corresponds to the radiating surface. A unit pressure must be used on both entries.

The uncoupled normal modes of the structure and fluid are computed with the SOL 103 solution sequence over a user-selected frequency range.

With the help of a DMAP script for PRIMODAL, the modes and surface loads along with the mesh are written to a set of output binary files, which are then imported to PRIMODAL for subsequent analysis.

### 3.3. PRIMODAL Analysis

The STL computation has been integrated in the SOLO module (SOund LOss) of PRIMODAL. The module includes the following features based on the theory presented in the previous chapter.

- STL computation using modal approach
- User-defined porous materials
- Generation of equivalent fluid models
- Reduced truncation error with residual modes
- Modal contributions to radiated power
- Element contributions to radiated power

These features are illustrated in the following industrial application.

## 4. INDUSTRIAL APPLICATION

### 4.1. Introduction

A panel structure with a porous cavity was used to assess and validate the STL computations in the SOLO module. The mesh is shown in Fig. 4 and comprises approximately 2000 nodes on each surface with a total surface area of 3 m2. The width of the cavity is approximately 45 mm.

The cavity was modelled in NASTRAN reference values corresponding to air.

The uncoupled modes were calculated up to 1000 Hz resulting in 403 structural modes and 1076 fluid modes along with the corresponding residual terms.

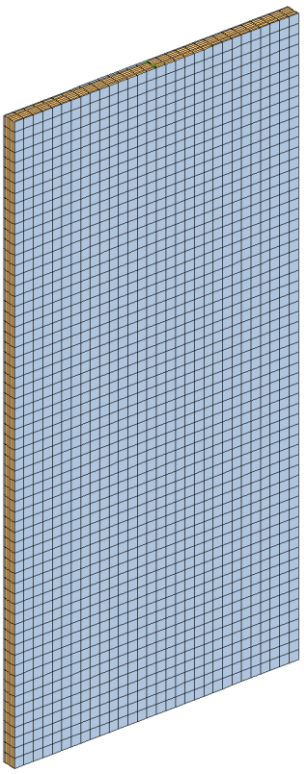

*Figure 4: Panel Structure with Porous Cavity*

### 4.2. Porous Model

Two analyses were carried out – one considering a non-porous cavity with only air, and a second with the addition of a porous material comparable to glass wool whose properties provide a high degree of damping of the acoustic cavity modes.

### 4.3. STL Computation

The STL for air and porous cavities are plotted in Fig. 5. The added damping of the porous material is significant over the entire frequency range starting with the first mode (antiresonance) at 23 Hz. Each STL calculation takes about 3 minutes for the 1000 frequency points.

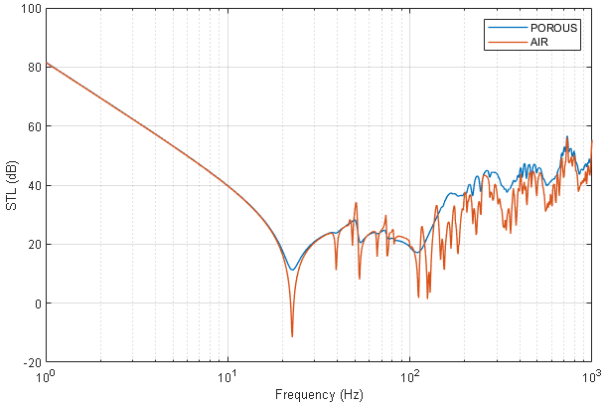


*Figure 5: STL with Air vs Porous Cavities*

Once the STL responses are caluated, the modal and surface contributions can be plotted for a given excitation frequency. The modal contributions are shown in Fig. 6 for the porous STL at 53.67 Hz. We

see that the modes 1 and 7 represent the principal contributions.

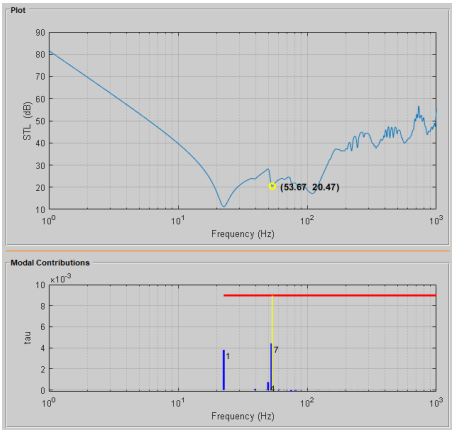


*Figure 6: STL Modal Contributions*

The contributions of the surface elements to the STL at 53.67 Hz are shown at left in Fig. 7. The corresponding surface element velocities are plotted at right.

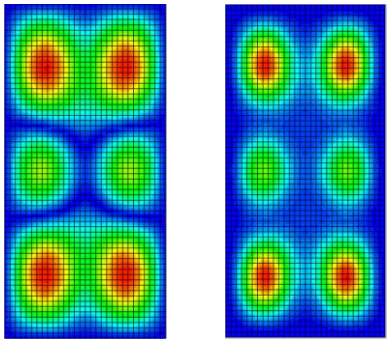

*Figure 7: STL and Velocity Distributions*

Validation of the STL calculation with porous cavities was carried by comparison with ACTRAN. An example comparison is provided in Fig. 8. The results are very close. The slight differences in the higher frequencies is probably due to the use of plane waves in ACTRAN to reproduce the diffuse field.

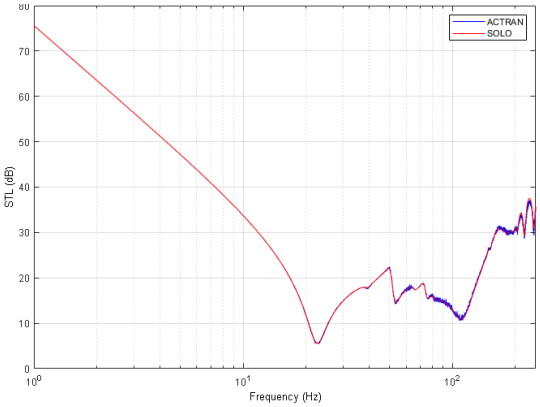


*Figure 8: STL Comparison ACTRAN vs SOLO*

## 5. CONCLUSIONS

A real mode approach to the computation of the sound transmission loss for panel structures with porous cavities has been implemented in an interactive software tool.

The porous cavities are modelled using an equivalent fluid model with frequency-dependent properties. The diffuse field is approximated by the blocked pressure using the joint acceptance functions. And the radiated sound power is computed using the Rayleigh integral. The use of these methods results in an efficient tool that can be of great use in preliminary design and optimization.

Additional features such as the modal and surface element contributions to the STL have been implemented.

## 6. REFERENCES

1. Séon, G., Roy, N., Vibro-acoustic Responses to Diffuse Acoustic Field using a Modal Approach and Application to the IXV Re-entry Vehicle Design Justification. *4th European Conference for Aerospace Sciences*, 2011.

2. Santiago-Prowald, J., Rodrigues, G., An Impedance/Mobility Condensation Method for Preliminary Vibro-Acoustic Analysis, *European Conference on Spacecraft Structures, Materials & Mechanical Testing,* Noordwijk, The Netherlands, 2005.

3. Witting, M., *Modelling of Diffuse Sound Field Excitations and Dynamic Response Analysis of Lightweight Structures*, Herbert Utz Verlag, Munich, Germany, 1999.

4. Coyette, J-P., Lielens, G., Power Indicators and Acoustic Diffuse Fields, *Free Field Technologies S.A*, 2009.

5. Koopmann, G. H., Fahnline, J. B., *Designing Quiet Structures – A Sound Power Minimization Approach*, Academic Press, 1997.

6. Putra, A. et al., Modelling sound radiation from a baffled vibrating plate for different boundary conditions using an elementary source technique, *InterNoise 2014,* Melbourne, Australia, 2014.

7. Bank, G., Wright, J. R., Radiation Impedance Calculations for a Rectangular Piston, *J. Audio Eng. Soc.,* Vol. 37, No. 5, May 1990.

8. Arenas, J. P., Numerical Computation of the Sound Radiation from a Planar Baffled Vibrating Surface, *Journal of Computational Acoustics.,* Vol. 16, No. 3, 2008.

9. Allard, J. F., Atalla, N., *Propagation of Sound In Porous Media – Modelling Sound Absorbing Materials*, Wiley, Second Edition, 2009.

10. Berger, S., *Contribution à la caractérisation des milieu poreux par des méthodes acoustiques : estimation des paramètres physiques*, Thèse de doctorat, Ecole Doctorale de l'Université du Maine, Le mans, 2004.